Letter

Purification timescales in monitored fermions

Hugo Lóio,[1,2] Andrea De Luca,[1] Jacopo De Nardis,[1] and Xhek Turkeshi[3]

[1]*Laboratoire de Physique Théorique et Modélisation, CNRS UMR 8089, CY Cergy Paris Université, 95302 Cergy-Pontoise Cedex, France*

[2]*CeFEMA, Instituto Superior Técnico, Universidade de Lisboa, Av. Rovisco Pais, 1049-001 Lisboa, Portugal*

[3]*JEIP, USR 3573 CNRS, Collège de France, PSL Research University, 11 Place Marcelin Berthelot, 75321 Paris Cedex 05, France*

(Received 29 March 2023; revised 18 July 2023; accepted 19 July 2023; published 28 July 2023)

We investigate the crucial role played by a global symmetry in the purification timescales and the phase transitions of monitored free fermionic systems separating a mixed and a pure phase. Concretely, we study Majorana and Dirac circuits with $\mathbb{Z}_2$ and U(1) symmetries, respectively. In the first case, we demonstrate the mixed phase of L sites has a purification timescale that scales as $\tau_P \sim L \ln L$. At $1 \ll t \ll \tau_P$ the system attains a finite residual entropy, that we use to unveil the critical properties of the purification transition. In contrast, free fermions with U(1) manifest a sublinear purification timescale at any measurement rate and an apparent Berezinskii-Kosterlitz-Thouless criticality. We find the mixed phase is characterized by $\tau_P \sim L^{\alpha(p)}$, with a continuously varying exponent $\alpha(p) < 1$.

DOI: 10.1103/PhysRevB.108.L020306

Introduction. Preparing pure states in many-body systems is fundamental for quantum simulation [1–3], metrology [4–8], and computation [9]. As a process, purification is regulated by the principles of thermodynamics. Left alone, quantum systems thermalize with the surroundings and reach a mixed state with extensive thermodynamic entropy [10–16]. The second law implies that purification requires the system to nonunitarily interact with an environment, while the third principle states that the time needed to prepare a zero entropy (pure) state diverges with the system size. This purification timescale is in principle dictated by the microscopic properties of the framework. Yet, it manifests a universal behavior, with the functional dependence on system size fixed by the system's dynamical phases. For instance, generic monitored many-body systems distinguish between mixed and pure phases, with the purification timescale exponential and logarithmic in system sizes, respectively [17–21]. Additionally, the purification timescale reveals a power-law divergence at the so-called measurement-induced phase transitions (MIPTs) governed by the underlying critical-field theory [22,23]. Overall, the properties of generic systems reflects in the phenomenology of entanglement propagation and transitions [22–84] with coinciding theoretical description in statistical mechanics [85–92].

On the other hand, the case of monitored free fermions is less understood. While the entanglement properties have been extensively discussed [93–111], purification has been only partially investigated. Reference [112] demonstrated that monitored fermionic systems are *not* generic as they purify at most quadratically (and not exponentially) in system size. However, this derivation does not account for the interplay between symmetry and locality in quantum systems. Indeed, local unitary operations scramble less compared to the global ones in Ref. [112], and thus are expected to shorten the purification timescales.

This Letter tackles these issues by investigating the prominent role of symmetry on monitored free fermions. Concretely, we investigate $\mathbb{Z}_2$ parity preserving or U(1) number-conserving circuits built of quadratic fermionic gates, the so-called *Gaussian circuits*. We unveil the purification timescale studying the entropy of an ancilla initially entangled with the system [19]. Irrespectively of the symmetry, frequent measurements drive the system in a *pure phase*, with purification time logarithmic in system size L. Instead, the purification timescale in the *mixed phase* at low measurement rates depends crucially on the system's symmetry. For $\mathbb{Z}_2$ symmetric circuits, we find $\tau_P \sim L \ln L$ supporting the recent analytical arguments based on the nonlinear sigma models (NLSMs) [113] (cf. also Refs. [114–116]). Consequently, the mixed phase preserves a residual thermodynamic entropy at $1 \ll t \ll \tau_P$ [117], enabling us to extract the correlation length critical exponent of the measurement-induced transition. Instead, U(1)-conserving circuits purify in a time *sublinear* in system size at any finite measurement rate. In the mixed phase, we find $\tau_P \sim L^{\alpha(p)}$ and continuously varying exponent $0 \leqslant \alpha(p) \lesssim 0.87$. As with the entanglement transitions [94,105], U(1) circuits reveal a Berezinskii-Kosterlitz-Thouless (BKT) measurement-induced transition separating the mixed and the trivial phase.

Purification transition in Gaussian circuits. We consider Gaussian circuits of free fermions with interspersed unitary-measurement discrete-time dynamics. Such a circuit is mappable to a random-tensor network [114,115], whose N-replica field theory is described by a nonlinear sigma model

$$\mathcal{S} = \frac{1}{2g_B} \int dx\, dt\, \mathrm{tr}(\partial^\mu Q)^T \partial_\mu Q + \ldots, \tag{1}$$

with $Q(x,t)$ an $N \times N$ matrix, g_B the bare coupling fixed by timescales of the microscopic model, N the number of replicas, and the ellipsis is on topological and symmetry-enlarged terms. We note that Eq. (1) applies also to Anderson localizing models [118–121], with the required replica limit $N \to 0$ instead of $N \to 1$ as in the measurement problem. Nevertheless, this draws an analogy between entanglement in

Gaussian circuits and conductance in disordered systems, with the running constant $g_R^{-1}(L)$ being a strength of entanglement (conductance) at a length scale L. Generic parity-conserving Majorana circuits correspond to the DIII Altland-Zirnbauer symmetry class [113,116], with beta function $dg_R/d\ln\ell \simeq (N-2)g_R^2/(8\pi) + O(g_R^3)$ known perturbatively at any N. We see here the importance of the correct replica limit, as the relevance of the flow is fixed by N. In particular, $N < 2$ implies a nontrivial stable phase governed by the $g_R \simeq 0$ fixed point [113], with the $N = 2$ limit corresponding to BKT behavior (cf. Ref. [114]).

The running coupling g_R affects entanglement and purification, as well as the universality class of the MIPT. Consider first a pure state $|\Psi\rangle$ and a bipartition $A \cup B$. The Rényi entropy $S_n(\rho) \equiv -\ln \mathrm{tr}(\rho^n)$ of the reduced density matrix $\rho_A \equiv \mathrm{tr}_B|\Psi\rangle\langle\Psi|$ measures the entanglement between A and B [122–124]. The running coupling $g_R^{-1} \simeq \ln L$ leads to the scaling in the entropy $S_n(\rho_A) \sim (n+1)/(96n)\ln^2 \ell_A$, with ℓ_A the length of A. The small prefactor hinders a precise entanglement scaling identification, which is susceptible to significant finite-size effects, resulting in conflicting numerical analysis [113,116]. An equivalent picture emerges from studying the purification of an initially mixed state ρ, revealed by the evolution of the S_2 of a monitored system [18,19,117]. While rigorous arguments upper bound the purification timescale of monitored free fermions to be quadratic in system size [112], the renormalized constant affects the purification timescale as $\tau_P \sim L/g_R(\ln L)$. In particular, for the DIII class, the analytic prediction is $\tau_P \sim L\ln L$ [113]. The advantage of considering the purification properties of the system is that they are extractable from a single ancilla qubit initially maximally entangled with the system [19,125,126], leading to practical experimental proxies [127,128] and more robust numerical checks compared to those based on entanglement measures. Including additional symmetries results in (potentially relevant) corrections to Eq. (1), altering τ_P.

We elaborate on these points by investigating $\mathbb{Z}_2$ parity-conserving and U(1) number-conserving systems. In the former case, the mixed phase purification timescale matches the NLSM prediction [113], indirectly supporting the flow $g_R \sim 1/\ln(L)$ for the DIII class circuits. Instead, the purification timescale is always sublinear in system size for the U(1) case, with a BKT transition separating trivial and mixed phases. The latter exhibits $\tau_P \sim L^{\alpha(p)}$ with continuously varying exponent $0 < \alpha(p) \lesssim 0.87$, supporting a running constant $g_R \sim L^{1-\alpha(p)}$. For concreteness, we discuss the implementations depicted in Fig. 1. The first example is based on an Ising Trotterization [cf. Fig. 1(a)]. Each layer is given by quadratic operations of Majorana fermions $\{\hat\gamma_a, \hat\gamma_b\} = 2\delta_{ab}$,

$$\hat K_p = \left[\prod_{j=1}^{L} \hat M_{2j-1,2j}^{r_j}\right]\left[\prod_{j=1}^{L} \hat U_{2j,2j+1}(J)\right]\prod_{j=1}^{L}\hat U_{2j-1,2j}(h), \quad (2)$$

where $r_j = 1$ with probability p, otherwise $r_j = 0$ and periodic boundary conditions apply. The probability p is one of the parameters of the model controlling the rate of measurements. The unitaries in Eq. (2) are fixed by $\hat U_{a,b}(\alpha) = \exp(-\alpha\hat\gamma_a\hat\gamma_b)$ and the on-site measurements act as

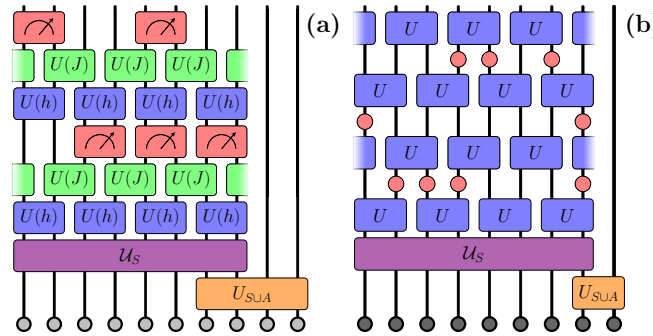

FIG. 1. Cartoon of the Gaussian circuits of interest. (a) The Majorana model with $\mathbb{Z}_2$ with three types of gates: on-site Floquet unitaries $\hat U(h)$ (blue), nearest-neighboring $\hat U(J)$ gates (green), and on-site measurements with probability p (red). (b) The stochastic U(1)-conserving model with $\hat U$ random gates (blue) and on-site measurements (red); cf. text. The gate $\hat U_{S\cup A}$ acts on the system and ancillae, while $\hat{\mathcal{U}}_S$ acts on the state. Varying them and the initial state, we uncover different but physically equivalent facets of the problem.

$$\hat M_{a,b}\rho\hat M_{a,b} = \frac{1}{p_\pm}\frac{1 \pm i\hat\gamma_a\hat\gamma_b}{2}\rho\frac{1 \pm i\hat\gamma_a\hat\gamma_b}{2} \quad (3)$$

with the sign randomly chosen according to the Born rule probabilities $p_\pm = (1 \pm \mathrm{tr}[i\hat\gamma_a\hat\gamma_b\rho])/2$ [129]. We infer the layer dependency on the measurement registry that fixed the quantum trajectory realization and call this system the Majorana circuit. The dynamics preserve the $\mathbb{Z}_2$ parity symmetry of the system.

Instead, the U(1) preserving dynamics is realized with a stochastic circuit of Dirac fermions $\{\hat c_a, \hat c_b^\dagger\} = \delta_{ab}$ with layers

$$\hat K_p^2 = \left(\prod_{j=1}^{L}\hat M_j^{r_j}\right)\prod_{i\in e}\hat U_{i,i+1}\left(\prod_{j=1}^{L}\hat M_j^{r_j}\right)\prod_{i\in o}\hat U_{i,i+1}, \quad (4)$$

with $i \in e/o$ running over even/odd sites. Periodic boundary conditions are assumed and $r_j = 1$ with probability p, otherwise $r_j = 0$. The unitary gates are given by $\hat U_{a,b} = \exp[-2i\beta(\hat c_a^\dagger\hat c_b + \mathrm{H.c.})]$ with β a random number in $[0,\pi]$ for each gate, while $\hat M_a$ is an on-site measurement of the particle density $\hat n_a = \hat c_a^\dagger\hat c_a$,

$$\hat M_a\rho\hat M_a = \begin{cases} \frac{\hat n_a\rho\hat n_a}{\mathrm{tr}(\hat n_a\rho)}, & \text{with probability } \mathrm{tr}(\hat n_a\rho) \\ \frac{(1-\hat n_a)\rho(1-\hat n_a)}{1-\mathrm{tr}(\hat n_a\rho)}, & \text{otherwise.} \end{cases}$$

Again we infer the measurement registry dependence of $\hat K_p$ and conveniently denote this as the Dirac circuit. This dynamics has a U(1) symmetry generated by the total fermionic number $\hat N = \sum_k \hat n_k$ [112].

The models of interest are simulatable with just polynomial complexity in system size as, by Gaussianity, the whole evolution reflects in the dynamics of the correlation matrix of the system [96,129]; respectively, $M_{a,b} = \mathrm{tr}(\rho i[\hat\gamma_a, \hat\gamma_b]/2)$ $(a,b = 1,\ldots,2L)$ and $C_{a,b} = \mathrm{tr}(\rho\hat c_a^\dagger\hat c_b)$ $(a,b = 1,\ldots,L)$ for the Majorana and Dirac circuits [130]. We study a complementary but physically equivalent framework, based on the system circuit evolution $\rho_{S\cup A}(t) = \hat K_{p,S}^t\rho_{S\cup A}(0)(\hat K_{p,S}^t)^\dagger$ of a system

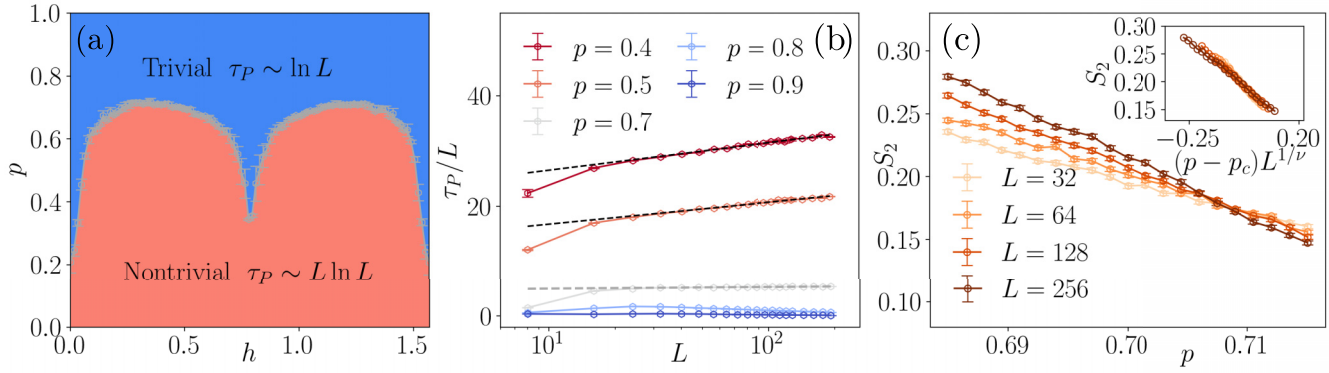

FIG. 2. (a) Phase diagram of the Majorana circuit. For $p < p_c(h)$, the system is in a nontrivial mixed phase characterized by a purification timescale $\tau_P \sim L \ln L$ (pink region). Instead, for $p > p_c$, the system is in the purified phase, with $\tau_P \sim \ln L$ (blue region). The critical line $p_c(h)$ is determined numerically and has the limit of $\tau_P \sim L$. (b) Scaling of the typical purification timescale τ_P with system sizes for various measurement rates. The dashed lines are logarithmic fits $f(x) = a \ln x + b$, with a, b two fitting parameters. The dashed gray line is a constant fit. (c) The residual entropy of an initially maximally mixed state at circuit depth $t = L$. Inset: data collapse with $p_c = 0.707$ and $\nu = 2.1$. In (b) and (c), $h = 0.3$.

and ancillae initial state $\rho_{S\cup A}(0) = \hat{\mathcal{U}}_S \hat{U}_{S\cup A} \rho_{0,S} \otimes \rho_{0,A} \hat{U}^\dagger_{S\cup A} \hat{\mathcal{U}}^\dagger_S$ (cf. Fig. 1). The latter is obtained from the uncorrelated initial density matrices $\rho_{0,S}$ and $\rho_{0,A}$ applying $\hat{U}_{S\cup A}$ and $\hat{\mathcal{U}}_S$, respectively, a system-ancillae unitary operation and a system unitary gate. Specifically, we consider (i) the purification of an ancilla system initially entangled to the system (with $\rho_{0,S/A}$ a product state, $\hat{U}_{S\cup A}$ a maximally entangling gate, and $\hat{\mathcal{U}}_S$ a scrambling gate) and (ii) the purification of a maximally mixed state (with $\rho_{0,S} = \mathbb{1}/2^L$ and $\hat{U}_{S\cup A}$, $\hat{\mathcal{U}}_S$ both identity gates, leaving the ancilla and system decoupled). In both instances, the purification properties are revealed by the residual entropy $S_2[\rho_S(t)]$. In particular, we extract the purification timescale τ_P from the former protocol as the characteristic timescale at which $S_2[\rho_S(t)] = 0$ [131].

Numerical results. We begin by numerically investigating the Majorana circuit [cf. Fig. 1(a)]. The results are summarized in the phase diagram in Fig. 2(a), where we fix $J = 0.5$. As we detail below, we find the critical line $p = p_c(h)$ in gray separating a nontrivial mixed phase for $p < p_c(h)$ (in red in the figure) and a purifying phase for $p > p_c(h)$ (in blue) studying the residual entropy. Note that the phase diagram is periodic with period π as a result of the choice of gates [cf. Eq. (2)], and here we show only one branch. In particular, we expect $p_c = 0$ as $h \to \pi$, since the $\hat{U}_{2j,2j-1}(h)$ become trivial.

We characterize the phases by first considering the purification of two Majorana ancillae, virtually located at the sites $L+1, L+2$ in Fig. 1(a). We initialize $\rho^{\text{majo}}_{S\cup A}(0)$ by locally entangling the ancillae with the system, and performing a scrambling operation on the system. The particular choice of scrambling operation does not change the qualitative physics (cf. [130]). We identify the purification timescale as $\tau_P = \text{median}(t_P)$, with $t_P = \min_t\{t : S_2[\rho_S(t)] < 10^{-10}\}$, and study its behavior for $\mathcal{N}_{\text{real}} > 10^3$ realizations of the circuit [132]. The results are reported in Fig. 2(b) at $h = 0.3$. In the mixed phase ($p < p_c \simeq 0.7$), we find $\tau_P \sim L \ln L$ as expected by the NLSM. Close to the critical value $p \approx p_c$, the system approaches a linear scaling $\tau_P \sim L$, while for $p > p_c$, the τ_P crosses over to $\sim \log L$ scaling. This logarithmic growth has a trivial origin and can be understood since the number of unmeasured sites must become $O(1)$ at $t \sim \tau_P$, i.e., $(1-p)^{\tau_P} L \lesssim 1$. The ancillae purification timescale, therefore, gives a clear separation between the trivial and mixed phases. This should be compared with the entanglement measures on extensive subsystems, where due to the significant finite-size effects, the identification of the scaling is more subtle (for instance, see discrepancies among Refs. [113,116]).

The superlinear τ_P in the mixed phase implies that the maximally mixed state $\rho_0 = \hat{\mathbb{1}}/2^L$ will sustain a residual entropy after a circuit evolution of depth $t \sim O(L)$. For such depths, the residual entropy $S_2 = \overline{S_2[\hat{K}^t_p \rho_0 (\hat{K}^t_p)^\dagger]}$ distinguishes a mixed phase, where it attains a finite value, from a trivial phase, where it is exponentially suppressed in system size. As an example, we present the results for $t = L$ and $h = 0.3$ in Fig. 2(c). Compatible with the single-qubit purification analysis, we observe a crossing behavior around $p \simeq 0.7$. This indicator estimates the p_c with $\lesssim 2\%$ interval of confidence already with limited system sizes [cf. Fig. 2(a)] where we consider $t = L \leqslant 64$ and averaging over 8000 trajectories. Nevertheless, obtaining the critical properties requires a finite-size scaling analysis, which we detail in [130], and gives $p^\star_c = 0.707(3)$ and $\nu^\star = 2.1(4)$. Our estimates, compatible with [115,117], lead to the data collapse in Fig. 2(c), inset. We see that the critical exponent is susceptible to more significant system size effects. We stress that an exact prediction for the exponent ν is not available even in the NLSM approach. The perturbative expansion around $N = 2$, where BKT scaling implies $\nu = \infty$, can nonetheless give a possible justification of its numerically large value [113]. A conclusive answer based solely on the numerics is, therefore, out of reach for the considered system sizes and demands more refined analytical insights.

We now investigate the purification of the Dirac circuit by considering the purification timescale of an ancilla maximally entangled with the system and virtually located at $L+1$ [cf. Fig. 1(b)]. Our numerical analysis is reported in Fig. 3. First, we find that for any p, the purification timescale is *sublinear* [cf. Fig. 3(a)]. As with the Majorana circuit, for $p \geqslant p_c \simeq 0.1$ the system has a logarithmic purification timescale set by the

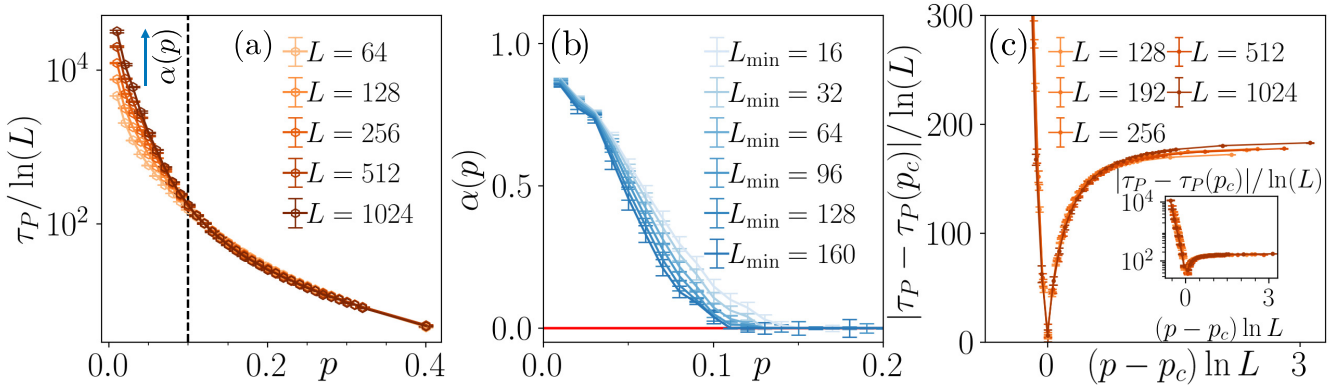

FIG. 3. (a) Purification timescale $\tau_P/\ln(L)$ for the Dirac circuit with U(1) for different system sizes $L \leqslant 1024$ and values of $p \in [0, 0.4]$. The critical rate p_c separates the mixed phase $p < p_c$, where one sees $\tau_P \sim L^{\alpha(p)}$ with $0 < \alpha(p) \lesssim 0.87$, from a purified phase $p > p_c$. (b) The continuously varying exponent $\alpha(p)$ is obtained considering larger system sizes for the fit (cf. text). For $p > p_c$ it is compatible to zero, while for $p < p_c$ it grows approaching $p \to 0$, saturating to a value $\sim$0.87. (c) The data collapse for a BKT finite-size scaling with the optimal $p_c = 0.10(1)$. Inset: same collapse but in log-log scale. We remark that the cost function minimization involves only a single fitting parameter.

scrambled initial state. In contrast, for $p \leqslant p_c$, the scaling is power law $L^{\alpha(p)}$, with an exponent $0 < \alpha(p) < 1$ which we extract from a fit [133]. To account for finite-size effects, we sequentially include only $L \geqslant L_{\min}$, with $L_{\min} = 16$–160 [cf. Fig. 3(b)]. For $p > p_c$, the result is compatible with $\alpha(p) = 0$, confirming the logarithmic system size scaling of τ_P. On the other hand, for $p < p_c$, the power-law exponent continuously varies with the rate p, and for $p \to 0$, it attains values close to $\alpha(0) \simeq 0.87$. This preliminary analysis demonstrates a more subtle phenomenology compared to the Majorana circuit, suggesting a scaling theory beyond the power-law diverging one of the NLSM. We, therefore, look for a BKT phase transition, where the correlation length diverges exponentially in $1/(p - p_c)$. Specifically, we consider the scaling variable $x = (p - p_c)\ln L$ and, to account for the logarithmic corrections at $p = p_c$, we perform the finite-size scaling on $\tau_P - \tau_P(p_c)$. In Fig. 3(c) we report the excellent data collapse, particularly when considering that the fit is performed with only one free parameter, p_c. The available system sizes support the hypothesis that U(1) number conservation leads to a measurement-induced phase transition in the BKT universality class for the Dirac circuits analyzed here as for the continuously monitored fermions [94,105]. In that case, $\alpha(p) \equiv z(p)$ would be a properly defined and continuously varying critical exponent $z(p)$, in line with a nonunitary Luttinger-liquid phase (cf. [105]). Nevertheless, we cannot exclude that the decrease in Fig. 3(b) continues and in the thermodynamic limit $\alpha(p) \to 0$ compatibly with possible weak-localization corrections (cf. [134]).

Conclusion. We analyzed the purification dynamics of monitored fermionic circuits, highlighting the role of symmetry in determining the purification timescales. For systems with a $\mathbb{Z}_2$ parity conservation, our results provide robust support to recent analytical arguments [113]. In particular, we find a purification timescale that increases as $\tau_P \sim L \ln L$ in the mixed phase. We benchmarked these results considering the residual entropy at $t = L \ll \tau_P$, demonstrating a phase transition signaled by a crossing in the finite-size scaling of S_2 and extracting the correlation length critical exponent. For systems with a U(1) conservation law, the purification timescale is sublinear in system size for any measurement rate and supports the presence of BKT stemming from the extended symmetry. Within the framework of NLSM introduced in [113], the available system sizes demonstrate this critical behavior separating a purifying phase from a mixed phase with $\tau_P \sim L^{\alpha(p)}$, indirectly supporting a running constant $g_R \sim L^{1-\alpha}$. We also note that the presence of a continuously varying exponent $0 \leqslant \alpha(p) \lesssim 0.87$ is compatible with previous studies on continuously monitored fermionic systems, as expected by virtue of universality.

In the continuous time limit, Ref. [105] found a BKT phase transition for U(1)-conserving fermions for the $N = 2$ replica. Nevertheless, Refs. [113,114,116] demonstrate the importance of the replica limit $N \to 1$ to determine the measurement-induced universal properties of the system, as well as the symmetry-permitted field theory corrections. It is important and left for further investigation to analytically demonstrate the robustness of the BKT measurement-induced transition in the correct replica limit, as well as the rightful characterization of the mixed phase purification timescales (cf. [134]) for a first step in this direction. Moreover, in line with Refs. [114,135], we expect that various discrete or continuous symmetries would enrich the phase diagram of the monitored system and leave hallmarks in the purification timescales. Lastly, our findings demonstrate the mixed phase of fermionic systems presents nontrivial structural properties that are revealable within the projective ensemble [136–143], for which the reduced density matrix reveals mean value properties.

Acknowledgments. We thank M. Fava, A. Nahum, and L. Piroli for the discussion on their recent results. J.D.N. thanks V. Alba, D. Rossini, and G. Piccitto for discussions. X.T. is indebted to B. Bauer, M. Buchhold, C.-M. Jian, A. W. W. Ludwig, and H. Shapourian for discussion on related topics, and thanks R. Fazio, M. Schirò, and P. Sierant for discussion and collaborations on related topics. He is supported by the ANR grant "NonEQuMat." (Grant No. ANR-19-CE47-0001) and computational resources on the Collge de France IPH

cluster. This work was granted access to the HPC resources of IDRIS under the allocation 2022-AD010513967, made by GENCI. J.D.N. and H.L. are supported by the ERC Starting Grant No. 101042293 (HEPIQ). A.D.L. acknowledges support by the ANR JCJC Grant No. ANR-21-CE47-0003 (TamEnt).

[1] I. M. Georgescu, S. Ashhab, and F. Nori, Rev. Mod. Phys. **86**, 153 (2014).
[2] K. J. Ferris, A. J. Rasmusson, N. T. Bronn, and O. Lanes, arXiv:2209.02795.
[3] J. Fraxanet, T. Salamon, and M. Lewenstein, arXiv:2204.08905.
[4] L. Pezzè, A. Smerzi, M. K. Oberthaler, R. Schmied, and P. Treutlein, Rev. Mod. Phys. **90**, 035005 (2018).
[5] J.-Y. Desaules, F. Pietracaprina, Z. Papić, J. Goold, and S. Pappalardi, Phys. Rev. Lett. **129**, 020601 (2022).
[6] S. Dooley, PRX Quantum **2**, 020330 (2021).
[7] S. Dooley, M. Hanks, S. Nakayama, W. J. Munro, and K. Nemoto, npj Quantum Inf. **4**, 24 (2018).
[8] S. Dooley, S. Pappalardi, and J. Goold, Phys. Rev. B **107**, 035123 (2023).
[9] J. Preskill, Quantum **2**, 79 (2018).
[10] J. M. Deutsch, Phys. Rev. A **43**, 2046 (1991).
[11] M. Srednicki, Phys. Rev. E **50**, 888 (1994).
[12] M. Srednicki, J. Phys. A **32**, 1163 (1999).
[13] M. Rigol, V. Dunjko, and M. Olshanii, Nature (London) **452**, 854 (2008).
[14] A. Polkovnikov, K. Sengupta, A. Silva, and M. Vengalattore, Rev. Mod. Phys. **83**, 863 (2011).
[15] L. Foini and J. Kurchan, Phys. Rev. E **99**, 042139 (2019).
[16] S. Pappalardi, L. Foini, and J. Kurchan, Phys. Rev. Lett. **129**, 170603 (2022).
[17] M. P. A. Fisher, V. Khemani, A. Nahum, and S. Vijay, Annu. Rev. Condens. Matter Phys. **14**, 335 (2023).
[18] M. J. Gullans and D. A. Huse, Phys. Rev. X **10**, 041020 (2020).
[19] M. J. Gullans and D. A. Huse, Phys. Rev. Lett. **125**, 070606 (2020).
[20] O. Lunt, M. Szyniszewski, and A. Pal, Phys. Rev. B **104**, 155111 (2021).
[21] P. Sierant, G. Chiriacò, F. M. Surace, S. Sharma, X. Turkeshi, M. Dalmonte, R. Fazio, and G. Pagano, Quantum **6**, 638 (2022).
[22] A. Zabalo, M. J. Gullans, J. H. Wilson, S. Gopalakrishnan, D. A. Huse, and J. H. Pixley, Phys. Rev. B **101**, 060301(R) (2020).
[23] P. Sierant, M. Schirò, M. Lewenstein, and X. Turkeshi, Phys. Rev. B **106**, 214316 (2022).
[24] O. Lunt, J. Richter, and A. Pal, Quantum simulation using noisy unitary circuits and measurements, in *Entanglement in Spin Chains: From Theory to Quantum Technology Applications*, edited by A. Bayat, S. Bose, and H. Johannesson (Springer, Cham, 2022), pp. 251–284.
[25] A. C. Potter and R. Vasseur, Entanglement dynamics in hybrid quantum circuits, in *Entanglement in Spin Chains: From Theory to Quantum Technology Applications*, edited by A. Bayat, S. Bose, and H. Johannesson (Springer, Cham, 2022), pp. 211–249.
[26] D. Rossini and E. Vicari, Phys. Rep. **936**, 1 (2021).
[27] A. Chan, R. M. Nandkishore, M. Pretko, and G. Smith, Phys. Rev. B **99**, 224307 (2019).
[28] Y. Li, X. Chen, and M. P. A. Fisher, Phys. Rev. B **100**, 134306 (2019).
[29] B. Skinner, J. Ruhman, and A. Nahum, Phys. Rev. X **9**, 031009 (2019).
[30] S. Czischek, G. Torlai, S. Ray, R. Islam, and R. G. Melko, Phys. Rev. A **104**, 062405 (2021).
[31] Y. Han and X. Chen, Phys. Rev. B **107**, 014306 (2023).
[32] Y. Minoguchi, P. Rabl, and M. Buchhold, SciPost Phys. **12**, 009 (2022).
[33] A. Altland, M. Buchhold, S. Diehl, and T. Micklitz, Phys. Rev. Res. **4**, L022066 (2022).
[34] Y. Fuji and Y. Ashida, Phys. Rev. B **102**, 054302 (2020).
[35] S.-K. Jian, Z.-C. Yang, Z. Bi, and X. Chen, Phys. Rev. B **104**, L161107 (2021).
[36] T. Jin and D. G. Martin, Phys. Rev. Lett. **129**, 260603 (2022).
[37] J. Willsher, S.-W. Liu, R. Moessner, and J. Knolle, Phys. Rev. B **106**, 024305 (2022).
[38] A. Pizzi, D. Malz, A. Nunnenkamp, and J. Knolle, Phys. Rev. B **106**, 214303 (2022).
[39] A. Lyons, S. Choi, and E. Altman, Phys. Rev. B **107**, 174304 (2023).
[40] L. Zhang, J. A. Reyes, S. Kourtis, C. Chamon, E. R. Mucciolo, and A. E. Ruckenstein, Phys. Rev. B **101**, 235104 (2020).
[41] P. Zhang, S.-K. Jian, C. Liu, and X. Chen, Quantum **5**, 579 (2021).
[42] P. Zhang, C. Liu, S.-K. Jian, and X. Chen, Quantum **6**, 723 (2022).
[43] T. Zhou and X. Chen, Phys. Rev. B **104**, L180301 (2021).
[44] G. S. Bentsen, S. Sahu, and B. Swingle, Phys. Rev. B **104**, 094304 (2021).
[45] Z.-C. Yang, Y. Li, M. P. A. Fisher, and X. Chen, Phys. Rev. B **105**, 104306 (2022).
[46] D. Rossini and E. Vicari, Phys. Rev. B **102**, 035119 (2020).
[47] R. Medina, R. Vasseur, and M. Serbyn, Phys. Rev. B **104**, 104205 (2021).
[48] O. Lunt and A. Pal, Phys. Rev. Res. **2**, 043072 (2020).
[49] S. P. Kelly, U. Poschinger, F. Schmidt-Kaler, M. P. A. Fisher, and J. Marino, arXiv:2210.11547.
[50] M. Szyniszewski, A. Romito, and H. Schomerus, Phys. Rev. B **100**, 064204 (2019).
[51] M. Szyniszewski, A. Romito, and H. Schomerus, Phys. Rev. Lett. **125**, 210602 (2020).
[52] Q. Tang and W. Zhu, Phys. Rev. Res. **2**, 013022 (2020).
[53] T. Iadecola, S. Ganeshan, J. H. Pixley, and J. H. Wilson, arXiv:2207.12415.
[54] N. O'Dea, A. Morningstar, S. Gopalakrishnan, and V. Khemani, arXiv:2211.12526.
[55] V. Ravindranath, Y. Han, Z.-C. Yang, and X. Chen, Phys. Rev. B **108**, L041103 (2023).
[56] L. Piroli, Y. Li, R. Vasseur, and A. Nahum, Phys. Rev. B **107**, 224303 (2023).

[57] P. Sierant and X. Turkeshi, Phys. Rev. Lett. **130**, 120402 (2023).
[58] S. Vijay, arXiv:2005.03052.
[59] R. Fan, S. Vijay, A. Vishwanath, and Y.-Z. You, Phys. Rev. B **103**, 174309 (2021).
[60] Y. Li, X. Chen, A. W. W. Ludwig, and M. P. A. Fisher, Phys. Rev. B **104**, 104305 (2021).
[61] M. Ippoliti, M. J. Gullans, S. Gopalakrishnan, D. A. Huse, and V. Khemani, Phys. Rev. X **11**, 011030 (2021).
[62] M. Ippoliti, T. Rakovszky, and V. Khemani, Phys. Rev. X **12**, 011045 (2022).
[63] K. Klocke and M. Buchhold, Phys. Rev. B **106**, 104307 (2022).
[64] T.-C. Lu and T. Grover, PRX Quantum **2**, 040319 (2021).
[65] M. Ippoliti and V. Khemani, Phys. Rev. Lett. **126**, 060501 (2021).
[66] Y. Li and M. P. A. Fisher, arXiv:2108.04274.
[67] Y. Li, R. Vasseur, M. P. A. Fisher, and A. W. W. Ludwig, arXiv:2110.02988.
[68] Y. Li, S. Vijay, and M. P. A. Fisher, PRX Quantum **4**, 010331 (2023).
[69] Y. Li and M. P. A. Fisher, Phys. Rev. B **103**, 104306 (2021).
[70] X. Feng, B. Skinner, and A. Nahum, arXiv:2210.07264.
[71] F. Barratt, U. Agrawal, A. C. Potter, S. Gopalakrishnan, and R. Vasseur, Phys. Rev. Lett. **129**, 200602 (2022).
[72] A. Zabalo, M. J. Gullans, J. H. Wilson, R. Vasseur, A. W. W. Ludwig, S. Gopalakrishnan, D. A. Huse, and J. H. Pixley, Phys. Rev. Lett. **128**, 050602 (2022).
[73] G. Chiriacó, M. Tsitsishvili, D. Poletti, R. Fazio, and M. Dalmonte, arXiv:2302.10563.
[74] P. Sierant and X. Turkeshi, Phys. Rev. Lett. **128**, 130605 (2022).
[75] J. Iaconis, A. Lucas, and X. Chen, Phys. Rev. B **102**, 224311 (2020).
[76] Y. Han and X. Chen, Phys. Rev. B **105**, 064306 (2022).
[77] H. Liu, T. Zhou, and X. Chen, Phys. Rev. B **106**, 144311 (2022).
[78] S. Sang, Y. Li, T. Zhou, X. Chen, T. H. Hsieh, and M. P. A. Fisher, PRX Quantum **2**, 030313 (2021).
[79] B. Shi, X. Dai, and Y.-M. Lu, arXiv:2012.00040.
[80] Z. Weinstein, Y. Bao, and E. Altman, Phys. Rev. Lett. **129**, 080501 (2022).
[81] X. Turkeshi, R. Fazio, and M. Dalmonte, Phys. Rev. B **102**, 014315 (2020).
[82] X. Turkeshi, Phys. Rev. B **106**, 144313 (2022).
[83] Z. Weinstein, S. P. Kelly, J. Marino, and E. Altman, arXiv:2210.14242.
[84] A. Zabalo, J. H. Wilson, M. J. Gullans, R. Vasseur, S. Gopalakrishnan, D. A. Huse, and J. H. Pixley, Phys. Rev. B **107**, L220204 (2023).
[85] S.-K. Jian, C. Liu, X. Chen, B. Swingle, and P. Zhang, Phys. Rev. Lett. **127**, 140601 (2021).
[86] J. Lopez-Piqueres, B. Ware, and R. Vasseur, Phys. Rev. B **102**, 064202 (2020).
[87] R. Vasseur, A. C. Potter, Y.-Z. You, and A. W. W. Ludwig, Phys. Rev. B **100**, 134203 (2019).
[88] C.-M. Jian, Y.-Z. You, R. Vasseur, and A. W. W. Ludwig, Phys. Rev. B **101**, 104302 (2020).
[89] A. Nahum, S. Roy, B. Skinner, and J. Ruhman, PRX Quantum **2**, 010352 (2021).
[90] A. Nahum and K. J. Wiese, arXiv:2303.07848.
[91] Y. Bao, S. Choi, and E. Altman, Phys. Rev. B **101**, 104301 (2020).
[92] S. Choi, Y. Bao, X.-L. Qi, and E. Altman, Phys. Rev. Lett. **125**, 030505 (2020).
[93] X. Cao, A. Tilloy, and A. D. Luca, SciPost Phys. **7**, 024 (2019).
[94] O. Alberton, M. Buchhold, and S. Diehl, Phys. Rev. Lett. **126**, 170602 (2021).
[95] T. Botzung, S. Diehl, and M. Müller, Phys. Rev. B **104**, 184422 (2021).
[96] X. Turkeshi, L. Piroli, and M. Schiró, Phys. Rev. B **106**, 024304 (2022).
[97] X. Turkeshi, A. Biella, R. Fazio, M. Dalmonte, and M. Schiró, Phys. Rev. B **103**, 224210 (2021).
[98] M. Buchhold, T. Müler, and S. Diehl, arXiv:2208.10506.
[99] T. Minato, K. Sugimoto, T. Kuwahara, and K. Saito, Phys. Rev. Lett. **128**, 010603 (2022).
[100] B. Ladewig, S. Diehl, and M. Buchhold, Phys. Rev. Res. **4**, 033001 (2022).
[101] G. Piccitto, A. Russomanno, and D. Rossini, Phys. Rev. B **105**, 064305 (2022).
[102] Y. L. Gal, X. Turkeshi, and M. Schiró, SciPost Phys. **14**, 138 (2023).
[103] E. Granet, C. Zhang, and H. Dreyer, Phys. Rev. Lett. **130**, 230401 (2023).
[104] T. Müller, S. Diehl, and M. Buchhold, Phys. Rev. Lett. **128**, 010605 (2022).
[105] M. Buchhold, Y. Minoguchi, A. Altland, and S. Diehl, Phys. Rev. X **11**, 041004 (2021).
[106] M. Coppola, E. Tirrito, D. Karevski, and M. Collura, Phys. Rev. B **105**, 094303 (2022).
[107] E. Tirrito, A. Santini, R. Fazio, and M. Collura, arXiv:2212.09405.
[108] X. Turkeshi, M. Dalmonte, R. Fazio, and M. Schirò, Phys. Rev. B **105**, L241114 (2022).
[109] A. Biella and M. Schiró, Quantum **5**, 528 (2021).
[110] X. Turkeshi and M. Schiró, Phys. Rev. B **107**, L020403 (2023).
[111] A. Nahum and B. Skinner, Phys. Rev. Res. **2**, 023288 (2020).
[112] L. Fidkowski, J. Haah, and M. B. Hastings, Quantum **5**, 382 (2021).
[113] M. Fava, L. Piroli, T. Swann, D. Bernard, and A. Nahum, arXiv:2302.12820.
[114] Y. Bao, S. Choi, and E. Altman, Ann. Phys. **435**, 168618 (2021).
[115] C.-M. Jian, B. Bauer, A. Keselman, and A. W. W. Ludwig, Phys. Rev. B **106**, 134206 (2022).
[116] C.-M. Jian, H. Shapourian, B. Bauer, and A. W. W. Ludwig, arXiv:2302.09094.
[117] J. Merritt and L. Fidkowski, Phys. Rev. B **107**, 064303 (2023).
[118] M. Bocquet, D. Serban, and M. Zirnbauer, Nucl. Phys. B **578**, 628 (2000).
[119] T. Senthil and M. P. A. Fisher, Phys. Rev. B **61**, 9690 (2000).
[120] J. T. Chalker, N. Read, V. Kagalovsky, B. Horovitz, Y. Avishai, and A. W. W. Ludwig, Phys. Rev. B **65**, 012506 (2001).
[121] F. Evers and A. D. Mirlin, Rev. Mod. Phys. **80**, 1355 (2008).
[122] L. Amico, R. Fazio, A. Osterloh, and V. Vedral, Rev. Mod. Phys. **80**, 517 (2008).
[123] P. Calabrese and J. Cardy, J. Stat. Mech. (2004) P06002.
[124] P. Calabrese and J. Cardy, J. Phys. A **42**, 504005 (2009).

[125] M. Block, Y. Bao, S. Choi, E. Altman, and N. Y. Yao, Phys. Rev. Lett. **128**, 010604 (2022).
[126] S. Sharma, X. Turkeshi, R. Fazio, and M. Dalmonte, SciPost Phys. Core **5**, 023 (2022).
[127] J. M. Koh, S.-N. Sun, M. Motta, and A. J. Minnich, Nat. Phys. (2023), doi:10.1038/s41567-023-02076-6.
[128] C. Noel, P. Niroula, D. Zhu, A. Risinger, L. Egan, D. Biswas, M. Cetina, A. V. Gorshkov, M. J. Gullans, D. A. Huse, and C. Monroe, Nat. Phys. **18**, 760 (2022).
[129] S. Bravyi, Quantum Inf. Comput. **5**, 216 (2005).
[130] See Supplemental Material at http://link.aps.org/supplemental/10.1103/PhysRevB.108.L020306 for details on the numerical implementation and additional numerical data, which includes Ref. [144].
[131] Indeed, in this case, the initial system-ancilla state is pure, $S_2[\rho_S(t)] = S_2[\rho_A(t)]$, allowing considerable simplification in the numerical calculations.
[132] *En passant*, we note that considering other indicators such as the average value give qualitatively similar results.
[133] To account for the logarithmic behavior for high rates $p \simeq 1$, we consider $f(x) = \beta(L^\alpha - 1)/\alpha$. *En passant*, we note that the available data cannot exclude the presence of multiplicative logarithms, arising in analogy to the $\mathbb{Z}_2$ case (cf. [130]).
[134] I. Poboiko, P. Pöpperl, I. V. Gornyi, and A. D. Mirlin, arXiv:2304.03138.
[135] K. Klocke and M. Buchhold, arXiv:2305.18559.
[136] J. S. Cotler, D. K. Mark, H.-Y. Huang, F. Hernández, J. Choi, A. L. Shaw, M. Endres, and S. Choi, PRX Quantum **4**, 010311 (2023).
[137] J. Choi, A. L. Shaw, I. S. Madjarov, X. Xie, R. Finkelstein, J. P. Covey, J. S. Cotler, D. K. Mark, H.-Y. Huang, A. Kale, H. Pichler, F. G. S. L. Brandão, S. Choi, and M. Endres, Nature **613**, 468 (2023).
[138] W. W. Ho and S. Choi, Phys. Rev. Lett. **128**, 060601 (2022).
[139] P. W. Claeys and A. Lamacraft, Quantum **6**, 738 (2022).
[140] M. Ippoliti and W. W. Ho, Quantum **6**, 886 (2022).
[141] M. Ippoliti and W. W. Ho, arXiv:2204.13657.
[142] M. Lucas, L. Piroli, J. De Nardis, and A. De Luca, Phys. Rev. A **107**, 032215 (2023).
[143] P. Łydzba, M. Mierzejewski, M. Rigol, and L. Vidmar, arXiv:2210.00016.
[144] N. Kawashima and N. Ito, J. Phys. Soc. Jpn. **62**, 435 (1993).